

Thermosensitive and Mucoadhesive Pluronic-Hydroxypropylmethylcellulose Hydrogel Containing the Mini-CD4 M48U1 Is a Promising Efficient Barrier against HIV Diffusion through Macaque Cervicovaginal Mucus

Kawthar Bouchemal,^a Armelle Aka-Any-Grah,^{a,b} Nathalie Dereuddre-Bosquet,^c Loïc Martin,^d Vanessa Lievin-Le-Moal,^e Roger Le Grand,^c Valérie Nicolas,^f Davide Gibellini,^g David Lembo,^h Christian Poüs,ⁱ Armand Koffi,^b Gilles Ponchel^a

Université Paris-Sud, Institut Galien Paris Sud, UMR CNRS 8612, Faculté de Pharmacie, Châtenay-Malabry, France^a; Université Félix Houphouët Boigny-Cocody, UFR des Sciences Pharmaceutiques et Biologiques, Laboratoire de Pharmacie Galénique, Biopharmacie et Législation, Abidjan, Côte d'Ivoire^b; CEA, IMETI, Division of Immunovirology, Fontenay-aux-Roses, France^c; CEA, iBiTecS, Service d'Ingénierie Moléculaire des Protéines (SIMOPRO), Gif sur Yvette, France^d; Antiparasitic Chemotherapy, UMR CNRS 8076, Faculté de Pharmacie, Châtenay-Malabry, France^e; Université Paris-Sud, IFR 141, Faculté de Pharmacie, Châtenay-Malabry, France^f; Department of Pathology and Diagnostic, Microbiology and Virology Unit, University of Verona, Verona, Italy^g; University of Turin, Department of Clinical and Biological Sciences, S. Luigi Gonzaga Hospital Regione Gonzole, Orbassano, Turin, Italy^h; Biochimie et Biologie Cellulaire-JE2493, Université Paris-Sud, IFR 141, Faculté de Pharmacie, Châtenay-Malabry, Franceⁱ

To be efficient, vaginal microbicide hydrogels should form a barrier against viral infections and prevent virus spreading through mucus. Multiple particle tracking was used to quantify the mobility of 170-nm fluorescently labeled COOH-modified polystyrene particles (COOH-PS) into thermosensitive hydrogels composed of amphiphilic triblock copolymers with block compositions EO_n-PO_m-EO_n (where EO refers to ethylene oxide and PO to propylene oxide) containing mucoadhesive hydroxypropylmethylcellulose (HPMC). COOH-PS were used to mimic the size and the surface charge of HIV-1. Analysis of COOH-PS trajectories showed that particle mobility was decreased by Pluronic hydrogels in comparison with cynomolgus macaque cervicovaginal mucus and hydroxyethylcellulose hydrogel (HEC; 1.5% by weight [wt%]) used as negative controls. Formulation of the peptide mini-CD4 M48U1 used as an anti-HIV-1 molecule into a mixture of Pluronic F127 (20 wt%) and HPMC (1 wt%) did not affect its anti-HIV-1 activity in comparison with HEC hydrogel. The 50% inhibitory concentration (IC₅₀) was 0.53 µg/ml (0.17 µM) for M48U1-HEC and 0.58 µg/ml (0.19 µM) for M48U1-F127-HPMC. The present work suggests that hydrogels composed of F127-HPMC (20/1 wt%, respectively) can be used to create an efficient barrier against particle diffusion in comparison to conventional HEC hydrogels.

According to the latest (2008) WHO and UNAIDS global estimates, among the 35 million people worldwide living with HIV, 50% are women. The first step in HIV infection by the vaginal route involves virus diffusion through vaginal mucus followed by the interaction of viral envelope proteins with their receptors on the surface of the vaginal host cells. Mucus is an entangled viscoelastic gel that coats the surfaces of the vaginal tract. It provides the outermost barrier against viral infections. The idea exposed in this work is to form a physical barrier composed of thermosensitive and mucoadhesive hydrogel against HIV diffusion, thus limiting virus attachment to mucosal surfaces of the vagina. The thermosensitive property of the (ethylene oxide)₉₈(propylene oxide)₆₇(ethylene oxide)₉₈ (EO₉₈PO₆₇EO₉₈) block copolymer designated Pluronic F127 or poloxamer P407 is particularly interesting for the design of vaginal microbicides acting as a physical barrier. At a certain concentration, this system is fluid at room temperature and in the form of a gel at body temperature (37°C) (1). In contrast to semisolid hydrogels, the administration of the formulation in the form of a solution (for instance, via syringes or another suitable device) facilitates its spreading on the mucosa, while the hydrogel layer on the mucosal surface could allow the formation of a physical barrier against virus diffusion. Mucoadhesion of Pluronic hydrogels was further improved by adding hydroxypropylmethylcellulose (HPMC) as a mucoadhesive polymer (1).

Previous works reported different techniques for the investigation of this barrier effect by using viruses or virus-like particles.

Diffusion chambers and Transwell-Snapwell chambers were used for hydrogel samples. The principle is based on donor-receptor duality. The sample containing the tracking substance, such as polystyrene particles, is placed in a donor chamber, and their passage in a receiver chamber filled with an appropriate liquid medium is observed (2, 3). However, this technique did not allow control of parameters such as thickness and uniformity of the sample layer, influence of preparation and handling on the structure of the sample, and optimal diameter of the pore to prevent blockage with the hydrogel sample (4). Fluorescence-labeled probe observations using fluorescence recovery after photobleaching (FRAP), single or multiple particle tracking (SPT or

Received 30 May 2014 Returned for modification 10 August 2014

Accepted 19 January 2015

Accepted manuscript posted online 2 February 2015

Citation Bouchemal K, Aka-Any-Grah A, Dereuddre-Bosquet N, Martin L, Lievin-Le-Moal V, Le Grand R, Nicolas V, Gibellini D, Lembo D, Poüs C, Koffi A, Ponchel G. 2015. Thermosensitive and mucoadhesive Pluronic-hydroxypropylmethylcellulose hydrogel containing the mini-CD4 M48U1 is a promising efficient barrier against HIV diffusion through macaque cervicovaginal mucus. *Antimicrob Agents Chemother* 59:2215–2222. doi:10.1128/AAC.03503-14.

Address correspondence to Kawthar Bouchemal, kawthar.bouchemal@u-psud.fr.

K.B. and A.A.-A.-G. were equally contributing authors.

Copyright © 2015, American Society for Microbiology. All Rights Reserved.

doi:10.1128/AAC.03503-14

MPT, respectively), and fluorescence correlation spectroscopy (FCS) are other techniques that present the advantage of being “soft techniques” without effect on the structure of the sample (5). These methods demonstrated the utility of using fluorescence techniques to study the transport and the stability of particles in different media. Particularly, single or multiple particle tracking can give information at individual particle scale, while the fluorescence laser-equipped microscope (FRAP) method gives ensemble-average data. These techniques are based on FRAP or photo diodes (FCS) as a light source and acousto-optic filters or modulators. For SPT, a fast and sensitive camera is added to the system. This camera permits analysis of dynamic phenomena like particle movements in a medium by showing each particle as a dot. The size of the dot is related to the resolution of the objective. It is possible to calculate particle positions with subresolution precision using algorithms that can calculate the centers of the dots (6).

The main objective of this work was to show that measuring the barrier effect of hydrogels is possible with soft techniques. We tried to correlate this barrier effect with Pluronic hydrogel intrinsic structure versus negative controls composed of macaque cervicovaginal mucus (CVM), hydroxyethylcellulose (HEC) hydrogel, and water. HEC hydrogel is very commonly used as a carrier of antiviral drugs in clinical studies on vaginal microbicides (7). Drug-free HEC hydrogel failed to prevent HIV transmission using macaque models (8, 9).

In the present work, multiple particle tracking was used to quantify the mobility of 170-nm fluorescence-labeled and negatively charged COOH-modified polystyrene particles (COOH-PS) into Pluronic-based hydrogels. COOH-PS were used to mimic the size and the surface charge of HIV-1. The size of HIV-1 virions ranges from 120 to 180 nm, while mature HIV-1 ranges from 140 to 220 nm (10). COOH-PS are negatively charged, thus mimicking the anionic HIV-1 virion envelope (4). Furthermore, multiple particle tracking showed that transport rates of COOH-PS are comparable to those of HIV in nonovulatory mucus (11).

Finally, the anti-HIV-1 activity of the mini-CD4 M48U1 formulated into hydrogels was evaluated. This peptide was used as an HIV-1 molecule that targets the initial step of viral attachment to the CD4 cell receptor to block the viral entry (12–14).

MATERIALS AND METHODS

Ethical statement. Adult cynomolgus macaques (*Macaca fascicularis*) were imported from Mauritius and housed in the facilities of the Commissariat à l’Energie Atomique et aux Energies Alternatives (CEA; Fontenay-aux-Roses, France). Nonhuman primates (NHP; including *M. fascicularis*) are used at the CEA in accordance with French national regulation and under national veterinary inspectors (CEA permit number A 92-032-02). The CEA is in compliance with Standards for Human Care and Use of Laboratory Animals of the Office for Laboratory Animal Welfare (OLAW, United States) under OLAW assurance number A5826-01. All experimental procedures were also conducted according to European guidelines for animal care (European directive 86/609, Journal Officiel des Communautés Européennes, L358, 18 December 1986). The use of NHP at CEA is also in accordance with recommendations in the newly published European Directive (2010/63, recommendation no. 9). No suffering was specifically associated with atraumatic vaginal fluid sampling in macaques. The animals were used under the supervision of the veterinarians in charge of the animal facility.

M48U1 synthesis. The M48U1 peptide containing a *p*-(cyclohexylmethyl)phenylalanine residue at position 23 was synthesized at Peptscan Presto Inc. (Lelystad, The Netherlands) by solid-phase peptide synthesis

and purified after refolding by reverse-phase high-performance liquid chromatography as described elsewhere (15). The M48U1 structure has been previously described (13).

Preparation of hydrogels. HEC hydrogel (percentage by weight [wt%], 1.5) was prepared by adding 1.5 g of gelling polymer HEC (Natrosol 250 M Pharm; Aqualon, USA) to a vial containing citrate buffer (5 mM, pH 4.5). The volume was then brought up to 100 g with citrate buffer. The final formulation was mixed with a mechanical stirrer until complete dissolution of HEC.

Pluronic-based hydrogels were prepared by weight according to the so-called cold method (1, 16, 17).

For the preparation of Pluronic-based hydrogels (F127 20 wt% and F127-F68, 22.5/2.5 wt%, respectively), Pluronic powders (BASF, Ludwigshafen, Germany) were gradually added under magnetic agitation at 4°C to citrate buffer. The different preparations were designated by two numbers indicating the weight percentages of Pluronic F127 and Pluronic F68, respectively.

For the preparation of formulations composed of F127-HPMC (20/*x* wt%) and F127-F68-HPMC (22.5/2.5/*x* wt%), HPMC powder (Methocel K4M series MM87091702 K; Colorcon) was gradually added under magnetic agitation at 4°C to citrate buffer. The proportion of HPMC in the formulation designated *x* was varied as 0, 0.2, 0.5, 0.8, and 1 wt%. After complete dissolution of HPMC, Pluronic powders were gradually added to this phase under the same conditions of temperature and agitation. Preparations composed of F127-F68-HPMC were denominated by three numbers indicating the percentages by weight of F127, F68, and HPMC, respectively.

Notably, F68 was added to modulate gelling temperature (T_{gel}), while HPMC was added to improve hydrogel mucoadhesion (1).

M48U1 (3 mg/g) was formulated by adding the peptide to hydrogels. The hydrogels were homogenized by magnetic mixing (18).

To investigate the effect of the pH on T_{gel} , the pH was adjusted to 7 using NaOH solution (Sigma-Aldrich, Saint-Quentin Fallavier, France).

In all cases, after complete dissolution of Pluronic powders, each formulation was hermetically sealed and stored for 48 h at 4°C to eliminate foam and air bubbles.

Rheological characterization of Pluronic-based hydrogels. All rheological measurements were carried out on a CSL 100 controlled-stress rheometer (Carri-Med; Rhéo Champlan, France). The geometry was a stainless steel cone/plate (diameter, 40 mm; angle, 2°; and gap, 54 μm), which provided homogeneous shear of the sample. The cone was equipped with a solvent trap to limit evaporation during measurement. Thanks to Pelletier diodes placed in the lower plate, it was possible to perform temperature sweeps from 0 to 70°C with a precision of 0.1°C. Oscillatory (or dynamic) experiments were carried out. A sinusoidal shear was applied to the sample where the stress $\tau(t)$ and the strain $\gamma(t)$ were defined as follows:

$$\tau(t) = \tau_0 \cos(\omega t) \quad (1)$$

$$\gamma(t) = \gamma_0 \cos(\omega t - \delta) \quad (2)$$

τ_0 and γ_0 are, respectively, the maximal amplitudes of the stress and strain, ω is $2\pi N$, N is the frequency, ω is the shear pulsation, and δ is the phase angle stress/strain.

From the phase angle, one could define various dynamic viscoelastic quantities and especially the elastic (or storage) modulus G' (equation 3) and the viscous (or loss) modulus G'' (equation 4).

$$G' = \frac{\tau_0}{\gamma_0} \cos \delta \quad (3)$$

$$G'' = \frac{\tau_0}{\gamma_0} \sin \delta \quad (4)$$

The higher the G' value, the more pronounced the elastic character, and conversely, the higher the G'' , the more pronounced the viscous properties.

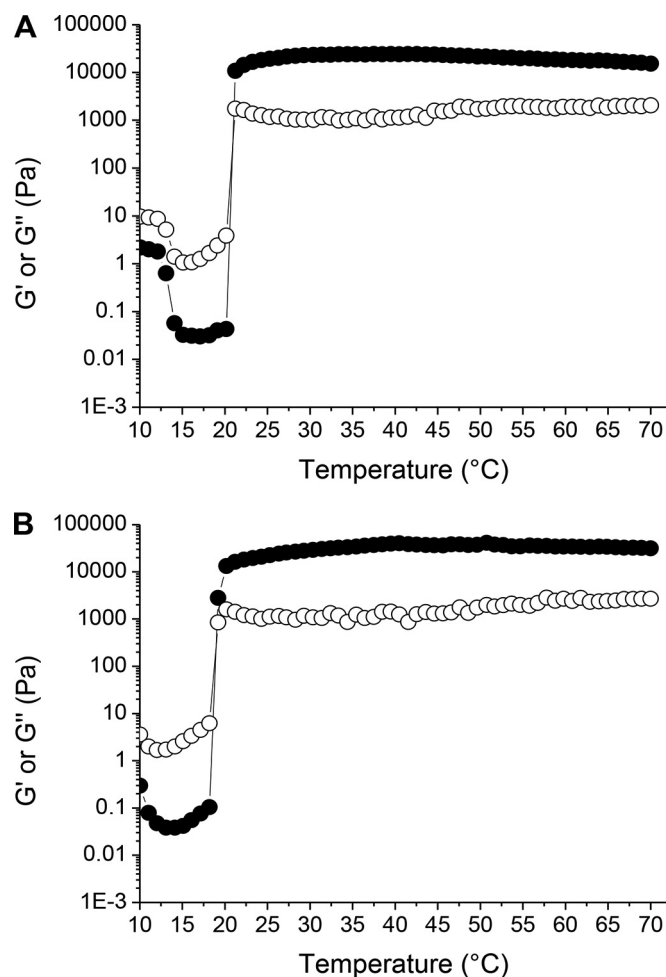


FIG 1 Typical profile of the variations of the elastic (G' , ●) and viscous (G'' , ○) moduli, as a function of temperature. Experiments performed with hydrogels composed of F127-HPMC (20/1 wt%, respectively) (A) and F127-F68-HPMC (22.5/2.5/1 wt%, respectively) (B).

Hydrogel dynamic viscosities (η) were calculated from the viscous modulus G'' according to equation 5:

$$\eta = \frac{G''}{2\pi} \quad (5)$$

Viscosities were evaluated at two different temperatures: (i) at 17°C, before gelification, all the formulations are in the form of viscous liquid; (ii) at 37°C, after gelification, the formulations are in the form of highly viscous gel.

The effect of HPMC addition on T_{gel} and η of Pluronic-based hydrogels was investigated after progressive addition of HPMC (0, 0.2, 0.5, 0.8, and 1 wt%) to hydrogels composed of F127 (20 wt%) and F127-F68 (22.5/2.5 wt%, respectively).

All rheological results are the means of $n = 3$ experiments.

Viscosity measurements of HEC hydrogel. Dynamic viscosity of HEC hydrogel was determined with an RS 600 controlled-stress rheometer (19) (Haake; Rhéo, France) at 25°C and 37°C. The geometry used was the stainless steel cone/plate (35/0.5°; truncation, 29 μ m), which provided homogenous shear of the samples and high values of the shear rate.

Evaluation of hydrogel cytotoxicity. Evaluation of hydrogel cytotoxicity was first conducted on HeLa cells (from UMR-S 756 Inserm and Université Paris-Sud, Faculty of Pharmacy, Châtenay-Malabry, France). The cells were grown in Dulbecco's modified Eagle's minimum essential medium (DMEM) with L-glutamine supplemented with 10% heat-inactivated fetal calf serum and 1% nonessential amino acids at 37°C in an atmosphere containing 5% CO₂. Cell lines were harvested from the flask using trypsin (0.5 mg/ml) with EDTA (0.2 mg/ml), washed once with culture medium, and seeded into culture plates at the appropriate cell densities (150,000 cells/well) before being incubated for 24 h at 37°C in an atmosphere containing 5% CO₂. For maintenance, cells were passaged weekly using 0.02% trypsin in Ca²⁺-Mg²⁺-free phosphate-buffered saline (PBS; 0.01 M, pH 7.4, at 25°C) containing 3 mM EDTA. The culture medium was changed every 2 days. Confluent HeLa cells were washed twice with PBS and then put in contact with hydrogels. The plates were incubated for 24 h at 37°C in a humidified atmosphere containing 5% CO₂. At the end of the contact period, cells were washed twice with sterile PBS before analysis. Quantification of viable cells was conducted with trypan blue enumeration in a Malassez cell.

Hydrogel cytotoxicity was also studied using the fully differentiated enterocyte-like Caco-2/TC7 clone cells (20, 21), and assays were performed on the mucin-secreting HT-29/MTX cell subpopulation (21, 22).

Caco-2/TC7 cells (from UMR-S 756 Inserm and Université Paris-Sud, Faculty of Pharmacy, Châtenay-Malabry, France) were grown in DMEM with 25 mM glucose, supplemented with 15% heat-inactivated fetal calf serum and 1% nonessential amino acids. HT-29/MTX cells (from UMR-S 756 Inserm and Université Paris-Sud, Faculty of Pharmacy, Châtenay-Malabry, France) were grown in DMEM (25 mM glucose) supplemented with 10% heat-inactivated fetal bovine serum. For maintenance, cells (Caco-2/TC7 or HT-29/MTX) were passaged weekly using 0.02% trypsin in Ca²⁺-Mg²⁺-free PBS containing 3 mM EDTA.

Experiments and cell maintenance for Caco-2/TC7 and HT-29/MTX were carried out at 37°C in an atmosphere containing 10% CO₂. The culture medium was changed daily. For Caco-2/TC7 cells, assays were performed with cells at passages between 15 and 32. Fully differentiated Caco-2/TC7 cells were obtained after 15 days in culture while HT-29/MTX cultures were used at late postconfluence after 21 days in culture. Evaluation of hydrogel cytotoxicity was achieved after 24 h of direct contact with the cells. Cells were prepared in 24-well culture plates at 75,000 cells/well for Caco-2/TC7 cells and at 125,000 cells/well for HT-29/MTX cells. Before contact with hydrogels, confluent cells were washed twice

TABLE 1 Effect of HPMC proportion (x wt%) on T_{gel} and η of hydrogels composed of F127 (20 wt%) or F127-F68 (22.5/2.5 wt%, respectively)^a

HPMC, x wt%	F127-HPMC (20/ x wt%, respectively)			F127-F68-HPMC (22.5/2.5/ x wt%, respectively)		
	T_{gel} (°C)	η (Pa/s) at:		T_{gel} (°C)	η (Pa/s) at:	
		17°C	37°C		17°C	37°C
0	22 ± 1	0.057 ± 0.001	101 ± 38	20 ± 1	0.259 ± 0.006	70 ± 22
0.2	21 ± 1	0.078 ± 0.001	105 ± 43	20 ± 1	0.335 ± 0.002	100 ± 3
0.5	21 ± 1	0.094 ± 0.002	108 ± 16	19 ± 1	0.453 ± 0.011	122 ± 48
0.8	20 ± 1	0.129 ± 0.003	122 ± 4	18 ± 1	0.650 ± 0.028	206 ± 90
1	21 ± 1	0.200 ± 0.015	172 ± 13	19 ± 1	0.710 ± 0.151	213 ± 15

^a $N = 1$ Hz. η was calculated from G'' according to the equation $\eta = G''/2\pi$. Data are the means of three determinations ± standard deviations.

TABLE 2 Effect of pH on T_{gel} of hydrogels composed of F127-HPMC or F127-F68-HPMC^a

pH	T_{gel} (°C)	
	F127-HPMC (20/1 wt%, respectively)	F127-F68-HPMC (22.5/2.5/1 wt%, respectively)
4.5	21 ± 1	20 ± 1
7	22 ± 1	21 ± 1

^a $N = 1$ Hz. Data are the means of three determinations ± standard deviations.

with PBS. The plates were incubated for 24 h at 37°C in a humidified atmosphere containing 10% CO₂. At the end of the contact period, cells were washed two times with sterile PBS before analysis.

Whatever the cell line used, citrate buffer and simulated vaginal fluid (SVF) were used as controls. SVF was prepared by adding (under stirring) 900 ml of distilled water contained in a beaker, NaCl (3.51 g), KOH (1.4 g), Ca(OH)₂ (0.22 g), bovine serum albumin (0.018 g), lactic acid (2.00 g), acetic acid (1.00 g), glycerol (0.16 g), urea (0.40 g), and glucose (5.00 g). The stirring was maintained until complete dissolution. The pH of the mixture was then adjusted to 4.5 using HCl, and the final volume was adjusted to 1 liter. All reagents for SVF preparation were from Sigma-Aldrich (Saint-Quentin Fallavier, France) and were of analytical grade.

Video microscopy and multiple particle tracking. Particle transport rates were measured by analyzing the trajectories of fluorescence-labeled carboxylate-modified polystyrene particles (COOH-PS; 170-nm size; PS-Speck Microscope Point Source kit yellow-green fluorescent beads from Invitrogen, Molecular Probes, Eugene, Oregon, USA) in the hydrogels (F127-HPMC, 20/1 wt%, respectively; F127-F68-HPMC, 22.5/2.5/1 wt%, respectively; HEC, 1.5 wt%) and in macaque CVM.

Macaque CVM was collected from 24 naive female cynomolgus macaques (*Macaca fascicularis*). The results were compared to the particle trajectories in water. Microscopic observations were made using an inverted AxioObserver Z1-Colibri (Zeiss, Germany) video microscope

equipped with a charge-coupled device (CCD) HSsm camera (9.9-μm pixel size) under optimal incubation conditions provided by an XL incubator. Time-lapse images were acquired with a Plan-Apochromat 63×/1.4-numerical-aperture (NA) oil-immersion objective lens, a 470-nm light-emitting diode (LED) for excitation, and a band-pass 505- to 550-nm filter to collect the emission of fluorescence. The data sets were processed using ImarisTrack 7.1.1 (Bitplane AG, Zurich, Switzerland) and Excel software. Experiments were carried out in 8-well glass chambers (Labtek, Campbell, CA), where 10 μl of 1/10-diluted particle solutions was added to 250 μl of Pluronic hydrogels, HEC hydrogel, macaque CVM, or water and incubated for 2 h at 37°C before microscopic observation. Trajectories of $n = 10$ particles were analyzed. Movies were captured with AxioVision 4.8 (Zeiss, Germany) software at a temporal resolution of 210 ms for 30 s. The coordinates of the particle centroid were transformed into time-averaged mean square displacements (MSDs) (equations 6 and 7) from which distributions of MSDs were calculated.

$$\Delta x_1(\Delta t) = x_2 - x_1 \quad (6)$$

where $x_1 = x(t_1)$, $x_2 = x(t_1 + \tau)$, and τ is a fixed time lag.

$$[\Delta r_1(\tau)]^2 = [\Delta x_1(\tau)]^2 + [\Delta y_1(\tau)]^2 \quad (7)$$

Evaluation of anti-HIV-1 activity of the formulations. HIV-1_{ada} strain (NIBSC, London, United Kingdom) stocks were prepared (23) in the lymphoblastoid T CD4⁺ C8166 cell line (a kind gift from Stefano Butò, ISS, Rome, Italy). All viral stocks were titrated using an HIV-1 gag p24 antigen enzyme-linked immunosorbent assay (ELISA) kit (bioMérieux, Marcy l'Etoile, France) at 1,000 ng/ml of the HIV-1 gag p24 protein. The peripheral blood mononuclear cells (PBMCs) were separated from healthy donor peripheral blood using a Ficoll gradient (Ficoll-Histopaque; Pharmacia, Uppsala, Sweden) and seeded in RPMI 1640 (Gibco, Gaithersburg, MD, USA) plus 10% fetal calf serum (Gibco) and 2 mM L-glutamine (Gibco) medium at 5×10^5 cells/ml. PBMCs were activated by phytohemagglutinin (PHA) (5 μg/ml; Sigma, St. Louis, MO, USA) plus interleukin-2 (IL-2) (10 U/ml; Pierce, Rockford, IL, USA) treatment for 72 h. The medium was replaced every 3 days with fresh medium.

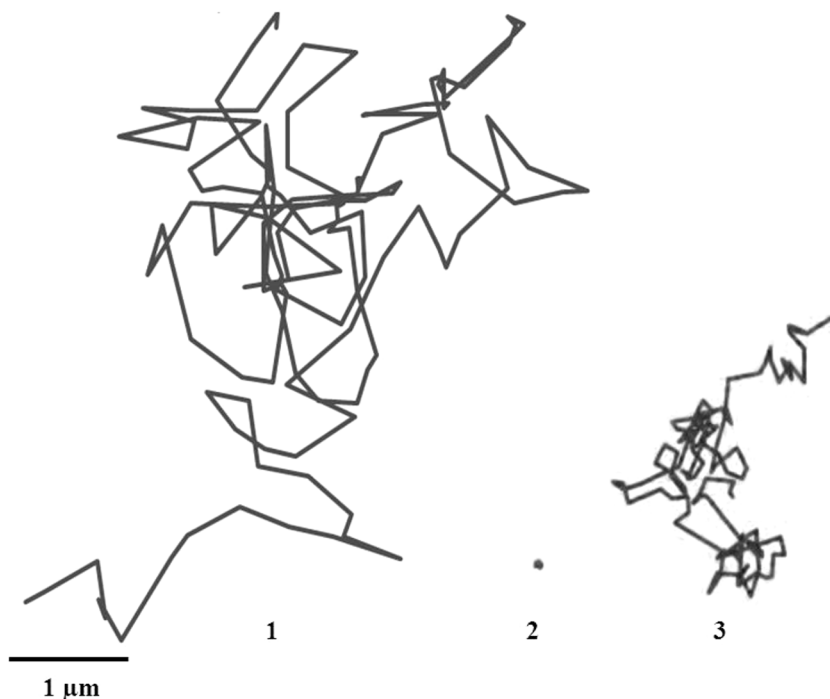


FIG 2 (1) Typical trajectories of fluorescence-labeled COOH-modified polystyrene particles in water. (2) Typical trajectory of fluorescence-labeled COOH-modified polystyrene particles that are stationary in CVM. (3) Trajectory of the particles that are mobile in CVM. The trajectories were obtained at 37°C.

Scalar concentrations of M48U1-HEC or M48U1-F127-HPMC were preincubated with the HIV-1_{ada} strain (5 ng/ml of HIV-1 gag p24) in RPMI 1640 for 1 h at 37°C or 4°C, respectively, and then added to PHA-IL-2-activated PBMCs that were adjusted to a final density of 1×10^6 cells/ml for 2 h at 37°C. Final M48U1 concentrations were 0.1, 1, 3, and 10 $\mu\text{g/ml}$. After four washes in PBS, cells were seeded at 1×10^6 PBMCs/ml into fresh medium represented by RPMI 1640 plus 10% fetal calf serum and 2 mM L-glutamine with scalar dilutions of either M48U1-HEC or M48U1-F127-HPMC. As control, the same protocol of preincubation was applied on untreated cultures or samples treated by relative hydrogel dilutions without M48U1. To analyze HIV replication, HIV-1 gag p24 content was evaluated at day 7 postinfection in culture supernatants using an HIV-1 p24 antigen ELISA kit (bioMérieux, Marcy l'Etoile, France). The PBMC viability was evaluated by trypan blue exclusion at day 7 using the same scalar concentrations of M48U1-HEC or M48U1-F127-HPMC indicated above. Untreated cell cultures were used as a control.

RESULTS AND DISCUSSION

Our strategy for the prevention of vaginal HIV transmission consists of the design of a barrier composed of Pluronic hydrogels containing the peptide mini-CD4 M48U1 able to better immobilize viral particles. This barrier could hinder HIV diffusion through mucus and its subsequent interaction with epithelial cells. Formulations composed of F127-HPMC (20 wt%) and F127-F68-HPMC (22.5/2.5/1 wt%, respectively) exhibited thermosensitive properties, evaluated by measuring the variation of elastic and viscous moduli when the temperature is progressively increased (Fig. 1). Both formulations are fluid at room temperature, facilitating their application and spreading within the vaginal cavity, while they form a highly viscous hydrogel above sol-gel transition temperature, promoting prolonged contact time with the vaginal mucosa at body temperature. We have previously demonstrated that addition of HPMC improved mucoadhesion of Pluronic hydrogels (1). HPMC addition did not have an impact on T_{gel} variation (Table 1).

The pH of Pluronic hydrogels was 4.5, within the range of the normal, premenopausal vaginal pH. During coitus, vaginal secretions are temporarily neutralized by the alkaline pH of semen. Results in Table 2 showed that T_{gel} was not significantly modified when the pH increased from 4.5 to 7.

In the present work, the ability of Pluronic hydrogels to decrease virus mobility was estimated by studying the trajectories of fluorescence-labeled carboxylate-modified polystyrene particles (COOH-PS; 170-nm size) using high-resolution multiple particle tracking in comparison with their movements in HEC hydrogel, CVM, and water, used as negative controls.

Particle mobility in water. The two-dimensional (2D) trajectories of COOH-PS in water exhibited a typical profile of the Brownian motion (Fig. 2, panel 1). The transport rates of different particle formulations in water were quantified by their time scale-dependent geometric ensemble-average mean square displacement (MSD) (Fig. 3). The slope α of each MSD curve was determined by fitting MSD to the equation $\text{MSD} = 4 D_0 \tau^\alpha$, where D_0 is the time scale-independent diffusion coefficient and τ is the time scale. α ranges from 0 for completely immobile particles to 1 for unobstructed Brownian diffusion, such as that of particles in water. Thus, a decrease of α value indicates increasing obstacles to particle movement. The slope of the MSD curves presented in Table 3 showed that α equals 1 as expected for pure unobstructed Brownian diffusion of particles in water.

Particle mobility in CVM. The analysis of COOH-PS trajec-

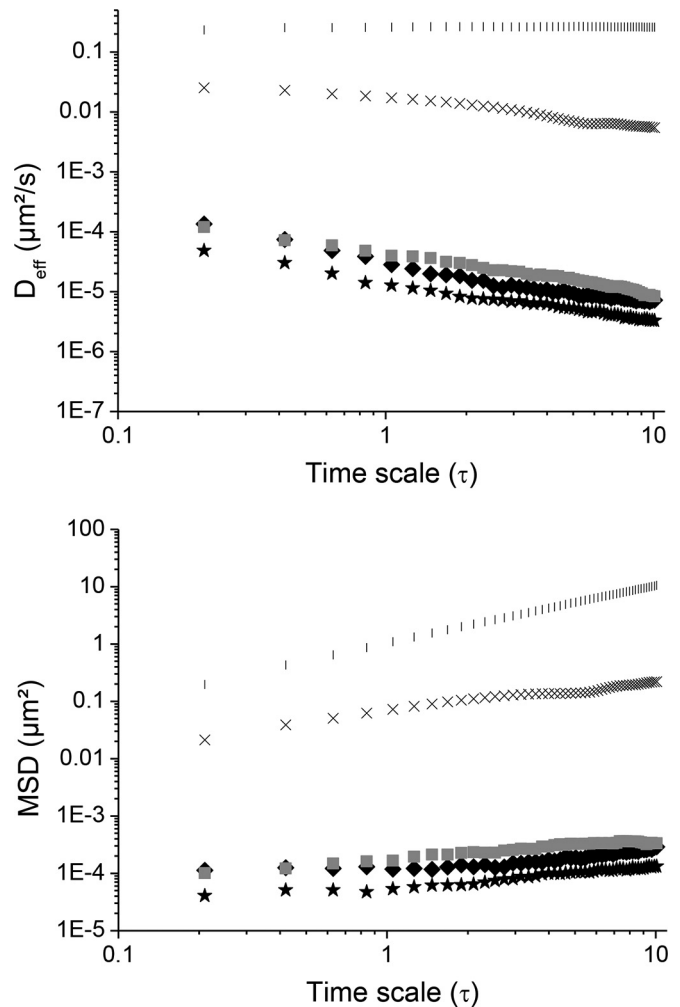


FIG 3 Comparison of average mean square displacements (MSDs) as a function of time scale of COOH-PS in water (○), HEC (1.5 wt%) (×), and macaque CVM (■) that are stationary in mucus, F127-HPMC (20/1 wt%, respectively) (★), and F127-F68-HPMC (22.5/2.5/1 wt%, respectively) (◆). The data were obtained at 37°C.

ries in CVM showed that 54% of particles were strongly slowed in mucus in comparison with water (Fig. 2, panel 2), while 46% of particles were not immobilized by mucus and exhibited Brownian or near-Brownian trajectories (Fig. 2, panel 3).

Mucus is mainly composed of water (95%) but also contains salts, lipids, enzymes, and proteins. The most important constituent of mucus is mucin. Mucin content usually ranges between 2 and 5% by weight. The immobilization of 54% of COOH-PS in mucus could be attributed to adhesive and low-affinity bonds of these particles with the hydrophobic domains of mucin.

The mobility of 46% of particles could be due to the heterogeneous structure of mucus and their diffusion through the large pores of mucus. Mucus pore size is heterogeneous, varying from 20 to 3,000 nm depending on the technique used. It was evaluated at 650 ± 150 nm using the freeze-substitution fixation technique and transmission electron microscopy (24). Scanning and transmission electron microscopy after dimethyl sulfoxide-mediated glutaraldehyde fixation evaluated the mesh spacing between mucin fibers at 20 to 200 nm (25, 26). More recently, mucus pore size was estimated to 340 nm by multiple particle tracking (27).

TABLE 3 Values of MSD, α , and D_{eff} of COOH-PS in different media^b

Sample	MSD μm^2 at 1 s	α	D_{eff} ($\mu\text{m}^2/\text{s}$) at 1 s	D_{eff}/D_w
Water	1.09	1	0.26	1
HEC (1.5 wt%)	0.07	56×10^{-3}	0.017	0.065
Macaque CVM ^a	1.66×10^{-4}	0.070×10^{-3}	3.95×10^{-5}	15.19×10^{-5}
F127-F68-HPMC (22.5/2.5/1 wt%, respectively)	1.18×10^{-4}	0.020×10^{-3}	2.80×10^{-5}	10.76×10^{-5}
F127-HPMC (20/1 wt%, respectively)	0.53×10^{-4}	0.009×10^{-3}	1.27×10^{-5}	4.88×10^{-5}

^a Data reported for particles stationary in mucus.

^b The slope α of each MSD curve was determined by fitting MSD to the equation $\text{MSD} = 4 D_0 t^\alpha$.

Particle trajectories in hydrogels. COOH-PS displacement was 16-fold lower in HEC than in water (Fig. 4, panels 2, and Table 3). The dynamic viscosity of HEC 1.5 wt% hydrogel determined at a shear rate of 0.1 s^{-1} was 3,200 mPa/s at 25°C and 1,900 mPa/s at 37°C, which is much higher than the dynamic viscosity of water (1 mPa/s at 25°C and 0.6947 mPa/s at 37°C) and could partly explain this reduced mobility.

Particles were strongly immobilized in both Pluronic hydrogels, F127-HPMC (20/1 wt%, respectively) and F127-F68-HPMC (22.5/2.5/1 wt%, respectively). This was evidenced by the highly constrained, non-Brownian time-lapse traces of COOH-PS observed in Fig. 4 (panels 3 and 4). The results at a time scale of 1 s showed that MSD and the average diffusivity of particles were 1,320- and 590-fold lower in F127-HPMC and F127-F68-HPMC hydrogels than in HEC (Table 3).

The higher dynamic viscosity of Pluronic hydrogels (Table 1) than of HEC hydrogel partly explains these differences. The two types of hydrogels are also different from a structural point of view. HEC is an ether of cellulose consisting of uncharged linear chains. Concerning Pluronic formulations, at low temperatures, before T_{gel} , copolymers exist in the form of unimers in low-viscosity aqueous solution. Upon heating, the dehydration of F127

unimers takes place and they begin to associate to form micelles composed of hydrophobic core formed by polypropylene oxide (PPO) blocks surrounded by the hydrophilic polyethylene oxide (PEO) blocks. When the temperature is increased above T_{gel} , Pluronic micelles arrange themselves in a well-organized crystalline structure. Small-angle X-ray diffraction experiments have shown that the diameter of each micelle was about 22 nm, and the distance between F127 20 wt% micelles was about 21 nm at a temperature higher than T_{gel} (28). This organization results from lower mobility of COOH-PS into Pluronic-based hydrogels than into HEC hydrogel.

The two types of Pluronic hydrogels, F127-HPMC and F127-F68-HPMC, exhibited different behaviors regarding the mobility of COOH-PS. This mobility was 2-fold higher in the hydrogel composed of F127-F68-HPMC than in the hydrogel composed of F127-HPMC. This result was unexpected because hydrogel composed of Pluronic mixture F127-F68-HPMC (22.5/2.5/1 wt%, respectively) was more viscous than hydrogel composed of F127-HPMC (20/1 wt%) at 37°C (Table 1). These findings suggest that high viscosity of hydrogels is not the main parameter controlling particle mobility. In a previous work conducted by our research group, the effect of F68 on the molecular organization of F127

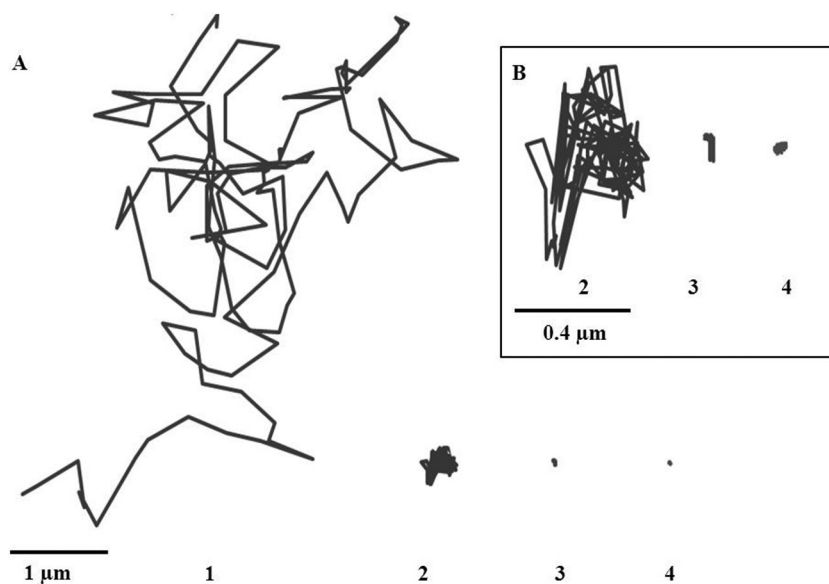


FIG 4 (A) Examples of trajectories of fluorescence-labeled COOH-modified polystyrene particles in water (1), HEC (1.5 wt%) (2), F127-F68-HPMC (22.5/2.5/1 wt%, respectively) (3), and F127-HPMC (20/1 wt%, respectively) (4). A close-up of panels 2, 3, and 4 is presented in panel B. The trajectories were obtained at 37°C.

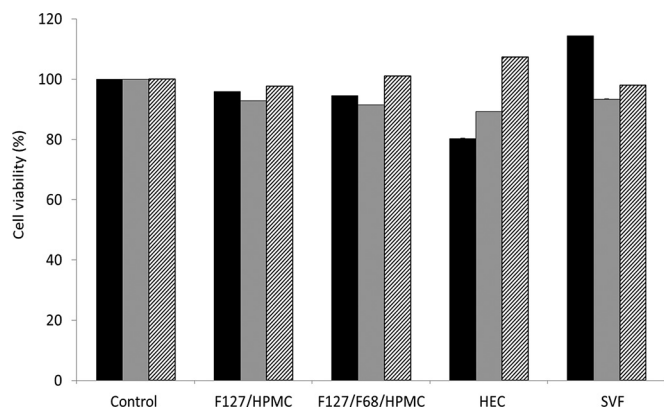


FIG 5 Percentages of cell viability of HeLa (black bars), Caco-2/TC7 (gray bars), and HT29-MTX (hatched bars) cells after 24 h of contact with F127-HPMC (20/1 wt%, respectively) and F127-F68-HPMC (22.5/2.5/1 wt%, respectively) hydrogels, in comparison with HEC and SVF. The control was composed of 5 mM citrate buffer, pH 4.5. Data are the means of three determinations \pm standard deviations.

micelles was studied (28). Micro-differential scanning calorimetry (micro-DSC) experiments unambiguously demonstrated that the two mixed Pluronic copolymers, F127 and F68, did not form mixed micelles but resulted in a segregation of the two kinds of copolymers (28). F68 is considered to be more hydrophilic than F127; its micellization temperature is higher. At 37°C, no micellization was detected at a concentration of F68 lower than 10 wt%. F127 formulations are more stable and more homogenous, while the presence of F68 results in a disruption of the crystalline structure of F127 micelles. This disorganization due to F68 resulted in a higher mobility of COOH-PS shown in Fig. 3 and 4.

These results clearly suggest that the relative efficiencies of hydrogels in hindering particle mobility are intimately related to their molecular structure. Hydrogel composed of F127 and HPMC is more suitable to be used as a physical barrier against HIV diffusion than the hydrogel composed of F127-F68 and HPMC.

Cytotoxicity. The nontoxicity of the hydrogels was demonstrated *in vitro* using HeLa cells (Fig. 5). HeLa cells are nonoriented cells derived from a human cervical carcinoma. Experiments evaluating hydrogel cytotoxicity were also conducted using the fully differentiated Caco-2/TC7 clone cells and the mucus-secreting HT-29/MTX cell subpopulation. Although Caco-2/TC7 cells are not derived from vaginal tissues, they were used here as a model of differentiated cells forming monolayers of polarized cells while HT-29/MTX cells were used as a mucus-secreting cell model. HT-29/MTX cells produce mucus secreted by the specialized goblet cells that cover the apical cell surface (for a review, see reference 29).

Whatever the cell model used, cell viability was found to be more than 80% for all samples. These results were in accordance with data from the literature on the toxicity of Pluronic hydrogels. Pluronic F127 has been approved by the FDA for use as a food additive and pharmaceutical ingredient. Moreover, Pluronic F127 hydrogel showed noncytotoxicity toward pig vaginal mucosa (30), indicating the biocompatibility of the Pluronic F127-based hydrogels reported here.

Anti-HIV-1 activity of hydrogels containing M48U1. The antiviral effect of scalar concentrations of M48U1-F127-HPMC was

TABLE 4 Antiviral activity of mini-CD4 M48U1 against HIV-1_{ada} infection^a

M48U1 concn, $\mu\text{g/ml}$ (μM)	HIV-1 gag p24 amt in medium:	
	M48U1-HEC	M48U1-F127-HPMC
0	100 \pm 10	100 \pm 8
0.1 (0.033)	85 \pm 9	83 \pm 9
1 (0.33)	37 \pm 6	42 \pm 6
3 (1)	4 \pm 2	6 \pm 2
10 (3.3)	2 \pm 1	3 \pm 2
IC ₅₀ , $\mu\text{g/ml}$ (μM)	0.53 (0.17 μM)	0.58 (0.19 μM)
95% CI, $\mu\text{g/ml}$	0.2010–1.441	0.1765–1.923

^a HIV-1_{ada} was preincubated for 1 h at 37°C or 4°C with scalar concentrations of M48U1-HEC or M48U1-F127-HPMC, respectively, in RPMI 1640 and challenged with activated PBMCs for 2 h at 37°C. HIV replication was monitored by HIV-1 gag p24 ELISA, and values were determined from cell culture supernatants at day 7 postinfection. Data were expressed as the means \pm standard deviations of HIV-1 gag p24 amount in relation to untreated control (set to 100%). Three experiments in duplicate were performed. IC₅₀, 50% inhibitory concentration; CI, confidence interval.

evaluated in comparison with M48U1-HEC (Table 4). The analysis of HIV-1 gag p24 content at day 7 postinfection in cell supernatants by ELISA demonstrated that M48U1 formulated into HEC or F127-HPMC hydrogels (3 to 10 $\mu\text{g/ml}$, 1 to 3.3 μM) effectively inhibits HIV infection (Table 4). Here, the effect of hydrogel formulation of M48U1 antiviral activity is investigated for the first time. The viability of activated PBMCs treated with M48U1-HEC or M48U1-F127-HPMC scalar concentrations with antiretroviral effects was not significantly affected compared with the untreated cell cultures (Fig. 6).

In conclusion, this investigation suggests that F127-HPMC (20/1 wt%, respectively) hydrogel could be suitable for use as a topical microbicide. Inclusion of an anti-HIV molecule in F127-HPMC (20/1 wt%, respectively) hydrogel represents an original strategy combining the effect of two barriers, mechanical and pharmacological, against HIV diffusion.

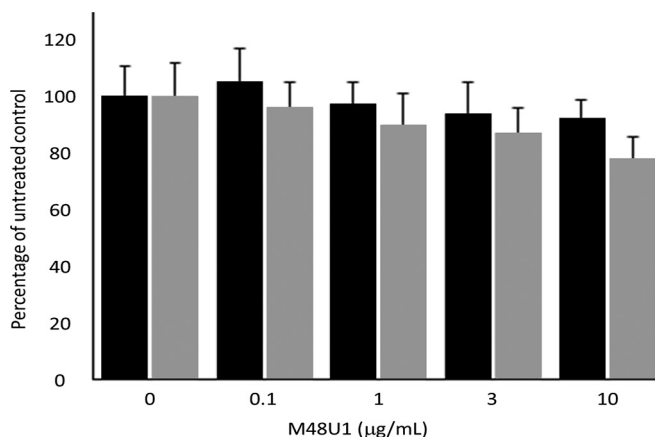


FIG 6 Trypan blue analysis of activated PBMC viability treated by scalar concentrations of M48U1-HEC (black bars) and M48U1-F127-HPMC (gray bars) at day 7. M48U1-HEC and M48U1-F127-HPMC at M48U1 concentrations with antiretroviral activity are not toxic for PBMCs. Data were expressed as the means (\pm standard deviations) of viable cells relative to untreated controls (set to 100%) obtained from three independent experiments in duplicate.

REFERENCES

- Aka-Any-Grah A, Bouchemal K, Koffi A, Agnely F, Zhang M, Djabourov M, Ponchel G. 2010. Formulation of mucoadhesive vaginal hydrogels insensitive to dilution with vaginal fluids. *Eur J Pharm Biopharm* 76:296–303. <http://dx.doi.org/10.1016/j.ejpb.2010.07.004>.
- Miyazaki M, Maeda H. 2006. Microchannel enzyme reactors and their applications for processing. *Trends Biotechnol* 24:463–470. <http://dx.doi.org/10.1016/j.tibtech.2006.08.002>.
- Sanders NN, De Smedt SC, Van Rompaey E, Simoens P, De Baets F, Demeester J. 2000. Cystic fibrosis sputum: a barrier to the transport of nanospheres. *Am J Respir Crit Care Med* 162:1905–1911. <http://dx.doi.org/10.1164/ajrccm.162.5.9909009>.
- Lai SK, Hida K, Shukair S, Wang YY, Cone R, Hope TJ, Hanes J. 2009. HIV is trapped by acidic but not by neutralized human cervicovaginal mucus. *J Virol* 83:11196–11200. <http://dx.doi.org/10.1128/JVI.01899-08>.
- Braeckmans K, Buyens K, Naeye B, Vercauteren D, Deschout H, Raemdonck K, Remaut K, Sanders NN, Demeester J, De Smedt SC. 2010. Advanced fluorescence microscopy methods illuminate the transfection pathway of nucleic acid nanoparticles. *J Control Release* 148:69–74. <http://dx.doi.org/10.1016/j.jconrel.2010.08.029>.
- Sbalzarini IF, Koumoutsakos P. 2005. Feature point tracking and trajectory analysis for video imaging in cell biology. *J Struct Biol* 151:182–195. <http://dx.doi.org/10.1016/j.jsb.2005.06.002>.
- Karim QA, Karim SSA, Frohlich JA, Grobler AC, Baxter C, Mansoor LE, Kharsany ABM, Sibeko S, Mlisana KP, Omar Z, Gengiah TN, Maarschalk S, Arulappan N, Mlotshwa M, Morris L, Taylor D. 2010. Effectiveness and safety of tenofovir gel, an antiretroviral microbicide, for the prevention of HIV infection in women. *Science* 329:1168–1174. <http://dx.doi.org/10.1126/science.1193748>.
- Tien D, Schnaare RL, Kang FR, Cohl G, McCormick TJ, Moench TR, Doncel G, Watson K, Buckheit RW, Lewis MG, Schwartz J, Douville K, Romano JW. 2005. *In vitro* and *in vivo* characterization of a potential universal placebo designed for use in vaginal microbicide clinical trials. *AIDS Res Hum Retroviruses* 21:845–853. <http://dx.doi.org/10.1089/aid.2005.21.845>.
- Dereuddre-Bosquet N, Morellato L, Brouwers J, Augustijns P, Bouchemal K, Ponchel G, Herrera C, Stefanidou M, Shattock R, Vanham G, Kessler P, Le Grand R, Martin L. 2012. MiniCD4 microbicide gel prevents vaginal transmission of SHIV162P3 in cynomolgus macaques. *PLoS Pathog* 8:e1003071. <http://dx.doi.org/10.1371/journal.ppat.1003071>.
- Briggs JAG, Wilk T, Welker R, Kräusslich H-G, Fuller SD. 2003. Structural organization of authentic, mature HIV-1 virions and cores. *EMBO J* 22:1707–1715. <http://dx.doi.org/10.1093/emboj/cdg143>.
- Lai SK, O'Hanlon ED, Harold S, Man ST, Wang YY, Cone R, Hanes J. 2007. Rapid transport of large polymeric nanoparticles in undiluted human cervical vaginal mucus. *Proc Natl Acad Sci U S A* 104:1482–1487. <http://dx.doi.org/10.1073/pnas.0608611104>.
- Martin L, Stricher F, Missé D, Sironi F, Pugniere M, Barthe P, Prado-Gotor R, Freulon I, Magne X, Roumestand C, Menez A, Lusso P, Veas F, Vita C. 2003. Rational design of a CD4 mimic that inhibits HIV-1 entry and exposes cryptic neutralization epitopes. *Nat Biotechnol* 43:71–76. <http://dx.doi.org/10.1038/nbt768>.
- Van Herwege Y, Morellato L, Descours A, Aerts L, Michiels J, Heyndrickx L, Martin L, Vanham G. 2008. CD4 mimetic miniproteins: potent anti-HIV compounds with promising activity as microbicides. *J Antimicrob Chemother* 61:818–826. <http://dx.doi.org/10.1093/jac/dkn042>.
- Stricher F, Huang CC, Descours A, Duquesnoy S, Combes O, Decker JM, Kwon YD, Lusso P, Shaw GM, Vita C, Kwong PD, Martin L. 2008. Combinatorial optimization of a CD4-mimetic miniprotein and cocystal structures with HIV-1 gp120 envelope glycoprotein. *J Mol Biol* 382:510–524. <http://dx.doi.org/10.1016/j.jmb.2008.06.069>.
- Martin G, Burke B, Thai R, Dey AK, Combes O, Ramos OHP, Heyd B, Geonnotti AR, Montefiori DC, Kan E, Lian Y, Sun Y, Abache T, Ulmer JB, Madaoui H, Guerois R, Barnett SW, Srivastava IK, Kessler P, Martin L. 2011. Stabilization of HIV-1 envelope in the CD4-bound conformation through specific cross-linking of a CD4 mimetic. *J Biol Chem* 286:21706–21716. <http://dx.doi.org/10.1074/jbc.M111.232272>.
- Koffi AA, Agnely F, Ponchel G, Grossiord J-L. 2006. Modulation of the rheological and mucoadhesive properties of thermosensitive poloxamer-based hydrogels intended for the rectal administration of quinine. *Eur J Pharm Sci* 27:328–335. <http://dx.doi.org/10.1016/j.ejps.2005.11.001>.
- Bouchemal K, Agnely F, Koffi A, Ponchel G. 2009. A concise analysis of the effect of temperature and propanediol-1,2 on pluronic F-127 micellization using isothermal titration microcalorimetry. *J Colloid Interface Sci* 338:169–176. <http://dx.doi.org/10.1016/j.jcis.2009.05.075>.
- Bouchemal K, Frelichowska J, Martin L, Liévin-Le-Moal V, Le Grand R, Dereuddre-Bosquet N, Djabourov M, Aka-Any-Grah A, Koffi A, Ponchel G. 2013. Note on the formulation of thermosensitive and mucoadhesive vaginal hydrogels containing the miniCD4 M48U1 as anti-HIV-1 microbicide. *Int J Pharm* 454:649–652. <http://dx.doi.org/10.1016/j.ijpharm.2013.02.055>.
- Mitri K, Vauthier C, Huang N, Menas A, Ringard-Lefebvre C, Anselmi C, Stambouli M, Rosilio V, Vachon J-J, Bouchemal K. 2012. Scale-up of nano-emulsion produced by emulsification and solvent diffusion. *J Pharm Sci* 101:4240–4247. <http://dx.doi.org/10.1002/jps.23291>.
- Chantret I, Rodolosse A, Barbat A, Dussaulx E, Brot-Laroche E, Zweibaum A, Rousset M. 1994. Differential expression of sucrose-isomaltase in clones isolated from early and late passages of the cell line Caco-2: evidence for glucose-dependent negative regulation. *J Cell Sci* 107:213–225.
- Fogh J, Fogh JM, Orfeo T. 1977. One hundred and twenty-seven cultured human tumor cell lines producing tumors in nude mice. *J Natl Cancer Inst* 59:221–226.
- Lesuffleur T, Barbat A, Dussaulx E, Zweibaum A. 1990. Growth adaptation to methotrexate of HT-29 human colon carcinoma cells is associated with their ability to differentiate into columnar absorptive and mucus-secreting cells. *Cancer Res* 50:6334–6343.
- Bon I, Lembo D, Rusnati M, Clò A, Morini S, Miserocchi A, Bugatti A, Grigolon S, Musumeci G, Landolfo S, Re MC, Gibellini D. 2013. Peptide-derivatized SB105-A10 dendrimer inhibits the infectivity of R5 and X4 HIV-1 strains in primary PBMCs and cervicovaginal histocultures. *PLoS One* 8:e76482. <http://dx.doi.org/10.1371/journal.pone.0076482>.
- Yudin AI, Hanson FW, Katz DF. 1989. Human cervical mucus and its interaction with sperm: a fine-structural view. *Biol Reprod* 40:661–671. <http://dx.doi.org/10.1095/biolreprod40.3.661>.
- Olmsted SS, Padgett JL, Yudin AI, Whaley KJ, Moench TR, Cone RA. 2001. Diffusion of macromolecules and virus-like particles in human cervical mucus. *Biophys J* 81:1930–1937. [http://dx.doi.org/10.1016/S0006-3495\(01\)75844-4](http://dx.doi.org/10.1016/S0006-3495(01)75844-4).
- Saltzman W, Radomsky ML, Whaley KJ, Cone RA. 1994. Antibody diffusion in human cervical mucus. *Biophys J* 66:508–515. [http://dx.doi.org/10.1016/S0006-3495\(94\)80802-1](http://dx.doi.org/10.1016/S0006-3495(94)80802-1).
- Lai SK, Wang Y-Y, Hida K, Cone R, Hanes J. 2010. Nanoparticles reveal that human cervicovaginal mucus is riddled with pores larger than viruses. *Proc Natl Acad Sci U S A* 107:598–603. <http://dx.doi.org/10.1073/pnas.0911748107>.
- Zhang M, Djabourov M, Bourgaux C, Bouchemal K. 2013. Nanostructured fluids from pluronic mixtures. *Int J Pharm* 454:599–610. <http://dx.doi.org/10.1016/j.ijpharm.2013.01.043>.
- Liévin-Le Moal V, Servin AL. 2013. Pathogenesis of human enterovirulent bacteria: lessons from cultured, fully differentiated human colon cancer cell lines. *Microbiol Mol Biol Rev* 77:380–439. <http://dx.doi.org/10.1128/MMBR.00064-12>.
- Pradines B, Bories C, Vauthier C, Ponchel G, Loiseau PM, Bouchemal K. 16 October 2014. Drug-free nanoparticles are active against *Trichomonas vaginalis* and non-toxic towards pig vaginal mucosa. *Pharm Res* <http://dx.doi.org/10.1007/s11095-014-1528-7>.